International Journal of Engineering

J o u r n a l   H o m e p a g e :   w w w . i j e . i r

Synthesis, Characterization, and Application of EDTA-Coated Maghemite Magnetic Nanoparticles for Oil Spill Cleanup from Water Surface

M. J. Awda*, B. A. Abdulmajeed

Department of Chemical Engineering, College of Engineering, University of Baghdad, Baghdad, Iraq

P A P E R I N F O	*A B S T R A C T*
	Oil spills pose significant environmental, ecological, and economic challenges worldwide. Since current remediation technologies proved inefficient in restoring marine ecosystems, this study adopted a straightforward and economical method of utilizing iron oxide magnetic nanoparticles. Maghemite (γ-Fe_2O_3) magnetic nanoparticles (MNPs) were synthesized using a homogeneous co-precipitation method. The colloidal dispersibility of MNPs was enhanced by applying an ethylene diamine tetra-acetic acid (EDTA) coating, resulting in a reduction of high surface energy and a subsequent decrease in nanoparticle agglomeration. MNPs were characterized using X-ray diffraction (XRD), Fourier transform infrared Spectroscopy (FTIR), transmission electron microscopy (TEM), scanning electron microscopy (SEM), energy-dispersive X-ray spectroscopy (EDX), and vibrating sample magnetometer (VSM). Removal experiments occurred at 25°C with a mass range of adsorbent (0.02-0.06 g). Oil-contaminated magnetic nanoparticles were extracted from the water surface by an external magnetic field using a neodymium magnet. The effects of both the oil API and the mass of adsorbent on gravimetric oil removal (GOR) were investigated. GORs for APIs 23, 28.4, and 40.3 were found to be 10.5±0.2-2.45±0.24, 8.96±0.18-1.15±0.06, and 5.11±015 to 1.01± 0.12g/g, respectively. Experimental results demonstrated an inverse relationship between GOR and the API value, indicating that as the API value decreased, GOR increased, and vice versa. Furthermore, as the mass of the adsorbent material was increased (0.02-0.06g), the GOR value decreased. The results of this study suggest that EDTA-maghemite MNPs have advantageous properties, including a small nanosize, super-paramagnetic behavior, and a large surface area. These characteristics make EDTA-maghemite a suitable sorbent for removing oil spills from water surfaces.

Graphical Abstract

* Corresponding Author Email: *maha.awda2107m@coeng.uobaghdad.edu.iq* (M. J. Awda)

1. INTRODUCTION

Water is an essential element for sustaining life on planet Earth. The aquatic ecosystem is experiencing significant contamination, resulting in the catastrophic degradation of natural watercourses (1-4). Several factors contribute to the problem of clean water shortage; one is the growing water demand, which is exceeding its supply, and another is the consequence of irresponsible human actions (5).

Due to the high global oil consumption, many countries rely heavily on oil as their main energy source and source of income (6). It is challenging to prevent oil spills. Millions of tons of energy were wasted as a result (7).

The release of oil into the environment presents significant hazards to both freshwater and marine ecosystems, impacting not just surface water supplies but also a diverse array of subsurface organisms interconnected within an intricate food chain, including vital human food sources (8).

Campos, Brazil (2011), Dalian, China (2010), and the Gulf of Mexico (2010), among numerous others., caused enormous destruction, proving the need for ongoing research into innovative remediation solutions (9). The Gulf of Mexico saw a very consequential oil spill, which is the most catastrophic incident of its kind. Approximately 750 million liters of oil were believed to have been discharged into the marine environment. In 2019, oil spread from Brazil's northeast and southeast, impacting about 2,000 kilometers of shoreline (10).

At the site of the oil spill, it is crucial to use both onshore and offshore oil response strategies, as well as continuous monitoring systems, to lessen the negative effects on the environment and human health. Numerous researchers have focused on mitigating oil spill incidents, aiming to limit the dispersion of pollutants and the subsequent complications (11).

Traditional oil spill cleanup strategies fall into four categories: (i) mechanical measures like booms and skimmers, (ii) chemical treatments like dispersants, (iii) in-situ burning, and (iiii) bioremediation. Various compounds, such as solidifiers and absorbents, have been utilized during these processes to clean up oil spills. The expensive cost and extended time required by these techniques are just two of their major drawbacks. Additional factors to consider are the secondary environmental pollution as a result of the materials used and the limited effectiveness of adsorption, especially when treating thin layers of oil (12, 13).

The oil sorption method is favored because of its many advantages, including its low energy requirements, low cost, excellent efficiency, and eco-friendlyness (14, 15).

Nanomaterials, including magnetic nanoparticles (MNPs), have attracted much interest as a sorbent for oil spills because of their beneficial properties (15, 16). These properties include easy separation and recovery through external magnetic fields, robust chemical, thermal, and mechanical stabilities, high surface area, ability to adsorb oil, and moderate saturation magnetization (17-19). Multiple methodologies exist that are recognized for the synthesis of MNPs, which include co-precipitation, hydrothermal, thermal decomposition, solvothermal, sol-gel, and microemulsion (20-24).

One of the most often employed and very efficient nanomaterials is known as SPIONs, which stands for super-paramagnetic iron oxide nanoparticles. These nanoparticles have a nanometer-sized iron oxide core that exhibits super hydrophobic properties (22, 25). Any compound containing iron, including oxides, hydroxides, and oxide-hydroxides, can be referred to as "iron oxide". Iron oxide has been found to exist in sixteen different phases; hence, differentiation between them can be achieved based on the inclusion of O_2 or the hydroxyl (OH) anions inside the crystalline framework (26).

The magnetic properties of SPIONs for oil recovery applications are their most attractive characteristics. Even though other MNPs, such as copper and nickel, among others, have similar magnetic properties (27). The majority of the literature points towards IONPs as the most promising, owing to low production costs, minimal toxicity, convenient synthesis and modification routes, and ease of magnetizing. Iron oxides that have been extensively researched in the domains of oil and gas are hematite (α-Fe_2O_3), magnetite (Fe_3O_4), and maghemite (γ-Fe_2O_3) (28, 29).

From a toxicological standpoint, SPIONs are considered toxic. However, relative to other MNPs, Fe_3O_4, and Fe_2O_3 have garnered much interest, especially in medical and pharmaceutical areas, because of their low toxicity and biological compatibility. They are distinctive because they are the only monocomponent metallic nanoparticles that the Food and Drug Administration (FDA) has approved (30). Therefore, they are employed in a variety of biological applications, including protein immobilization, MRI, thermal therapy, and drug administration (31-33).

Due to its extensive research, maghemite (γ-Fe_2O_3) is considered a desirable material for several applications such as medicationin drug delivery, data storage, catalysts, bioseparation, and magnetic sensors (34, 35). There are two advantages to use maghemite (γ-Fe_2O_3) in water treatment applications. It is a superior contaminant remover due to the combination of its magnetic and photocatalytic characteristics. Maghemite, also known as oxidized magnetite, is classified as an n-type

semiconductor due to its electronic properties. It is categorized as a ferromagnetic oxide and exhibits a spinel structure that closely resembles that of magnetite (36). Many contaminants, including those in aqueous solutions, drinking water, effluent, groundwater, and acid mine drainage, have been effectively extracted from water samples through the utilization of Maghemite MNPs, which may be incorporated into nanocomposites, surface-modified, or in their original, unadulterated state. The adsorption efficiencies of these Maghemite MNPs have been shown to be quite high, reaching close to 100% for certain contaminants (29, 37).

The inevitability of the long-term instability of particles within this specific size range is apparent. These particles prefer to seek agglomerates in order to lower the energy associated with nanoparticles' greater surface-area-to-volume ratio (38). Due to their chemical reactivity and susceptibility to air oxidation process, the nanoparticles exhibit diminished magnetic properties and dispersibility (39). Developing protective measures to chemically stabilize bare magnetic nanoparticles against degradation throughout or subsequent to the production process is critical for many applications. Incorporating organic species such as surfactants or polymers by grafting, as well as applying an inorganic layer such as silica or carbon coating, are among the methodologies employed (40).

Many studies have shown that ethylene diamine tetra-acetic acid (EDTA) has a strong affinity for iron oxide nanoparticles, which might make it easier for colloids to spread out, lower high surface energy, and stop nanoparticles from sticking together (41-44).

In this study, since no reports of oil spill recovery using coated maghemite (γ-Fe$_2$O$_3$) with EDTA as an adsorbent have been published, pure maghemite MNPs were synthesized and coated with EDTA to investigate their efficiency for adsorbing crude oil from the water surface using the gravimetric method with different doses of coated MNPs. Three Iraqi crude oils with different APIs and artificial seawater (35% Nacl) were employed to simulate an oil spill.

2. MATERIALS AND METHOD

2. 1. Materials   The materials used in this study included the following: All chemicals were of analytical reagent grade and were utilized without further treatment. Ferric chloride hexahydrate (FeCl$_3$.6H$_2$O 99%), ferrous chloride tetrahydrate (FeCl$_2$.4H$_2$O 98%), Urea (CO(NH$_2$)$_2$) and Ethylene diamine tetra-acetic acid (EDTA, C$_{10}$H$_{18}$N$_2$O$_8$, 99%) from CDH (India), ammonium hydroxide solution (NH$_4$OH, 25% of ammonia) from BDH Chemicals (England).

Crude oil, which was taken from Al-Dura Refinery (Basrah crude oil) (Location: EBS-OM-S2 Site) and (Naft Khana) in Iraq, their properties are displayed in Table 1.

TABLE 1. Crude oils properties

Property	Basrah Crude Oil	Naft Khana	East Baghdad S2
Sp.Gr. at 15.6°C	0.88490	0.823	0.9158
API	28.40	40.3	23
Viscosity (cp) at 26.7°C	19.4	3.056	8.505

2. 2. γ-Fe$_2$O$_3$ Preparation γ-Fe$_2$O$_3$MNPs were produced utilizing a homogeneous co-precipitation technique as described (45). At room temperature, 6.16 g of FeCl$_2$.4H$_2$O and 16.75 g of FeCl$_3$.6H$_2$O were added to (1.5g) urea in 100 mL of deionized water. Subsequently, the solution was gradually heated up to 80°C for 1 hour under reflux circumstances to decompose the urea.

After one hour, a diluted ammonia solution was introduced into the combined solution to adjust its pH to around 10.5. This adjustment was carried out while the solution was being stirred. An additional 30 minutes of reflux at a temperature of 80°C.

During the progression of the reaction, the formation of a precipitate with a reddish-brown color is perceived. After cooling to ambient temperature, the reddish-brown precipitate was subsequently isolated and subjected to a thorough washing procedure involving three cycles of deionized water rinsing to effectively remove any remaining residues resulting from the reaction.

Later, the specimen underwent two rounds of cleansing using acetone and was subsequently air-dried at ambient conditions.

2. 3. Coating with EDTA   EDTA was used to coat γ-Fe$_2$O$_3$ MNPs. After adding 0.615 g of EDTA to a solution of 4.48 g of MNPs in water, the suspension was agitated for 1 hour at 50°C (46). The precipitates were separated magnetically. The solution was rinsed with deionized water until its pH was adjusted to 7.

Subsequently, the precipitate was dispersed in 200 mL of deionized water and subjected to ultrasonic treatment for 30 minutes. The resulting product consisted of a black precipitate of EDTA-MNPs, which was separated from the liquid phase and subsequently subjected to drying at a temperature of 80°C for a duration of 3 hours. The dried material was then pulverized using a mortar.

2. 4. Characterization Techniques   The generated magnetic nanoparticles (MNPs) underwent characterization using XRD analysis. This analysis used an X-ray diffractometer (Shimadzu SRD 6000, Japan) with specific parameters, including a two-theta range of 10-80. This characterization aimed to confirm the structure and presence of the maghemite phase in the MNPs.

The TEM investigation used the electron microscopy instrument (EM 900, Zeiss). The SEM pictures were

acquired using the Oxford instrument model TE SCAN, Vega III lm-CZECK. The surface area was quantified with the Brunauer-Emmett-Teller (BET) technique., employing a micrometric ASAP 2020 equipment.

The magnetism at room temperature was measured using a VSM, MDK6). The Fourier transform infrared (FTIR) study was conducted using an IRPrestige-21 Fourier transform infrared spectrophotometer manufactured by Shimadzu, Japan. The scan range employed was from 4000 to 400 cm^{-1}. This analysis aimed to verify the presence of the maghemite phase and ascertain that the magnetic nanoparticles (MNPs) were coated with EDTA.

2. 5. Oil Removal Experiment   The investigation on oil removal was conducted utilizing the GOR technique, as previously documented (47). An (80 mL) solution of artificial seawater containing 3.5% sodium chloride (NaCl) was carefully poured into a 100 mL beaker. A quantity of crude oil (API 23, 28.4, 40.3) weighing 0.2 g was dropped into the water surface.

Subsequently, a measured amount of EDTA- γ Fe$_2$O$_3$ weighing 0.02-0.06 g was evenly distributed over the oil spill. The EDTA- (MNPs) in the oil were retrieved using a permanent magnet after 5 minutes. Figure 2 demonstrates the process of simulating an oil spill (i.e., placing the oil samples on the water surface and resulting in two distinct phases that simulate an oil spill without emulsification), the adsorption of the oil by EDTA-MNPs, and the removal of the oil-laden MNPs from the water surface using an external magnetic field. The oil removal experiments were carried out in triplicate, and Equation 1 was utilized to measure the GOR, g/g.

$$GOR = \frac{m_2 - m_3}{m_1} \tag{1}$$

The variable m_1 represents the mass of adsorbent, m_2 represents the total mass of the beaker, encompassing the oil spot, adsorbent, and water. Alternatively, m_3 denotes the mass of the leftover oil (the mass of the beaker after the removal).
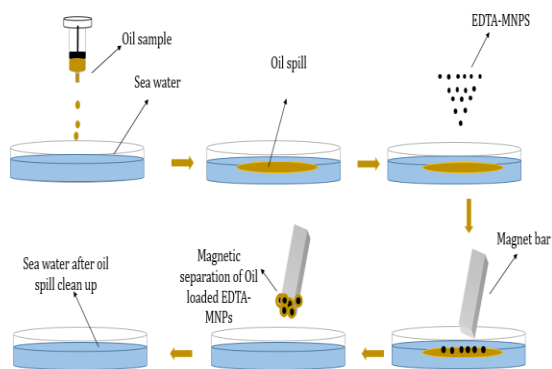
3. RESULTS AND DISCUSSION

3. 1. Characterization   The crystal structure of gamma-Fe$_2$O$_3$ resembles that of Fe$_3$O$_4$; however, cation vacancies are specifically located in the octahedral location within the spinel lattice. Two distinct crystalline phases, namely the disordered and ordered phases, can be observed depending on whether the cations and vacancies exhibit ordering or not. Typically, the synthesis techniques employed at low temperatures tend to form the disordered phase, according to the study conducted by Sreeja and Joy (48).

The crystal structures of γ-Fe$_2$O$_3$ were analyzed using XRD techniques, which provided evidence for the presence of the maghemite phase. Figure 3 illustrates the XRD patterns of MNPs, which give evidence of the maghemite γ-Fe$_2$O$_3$ possessing a very crystalline structure. The observed peaks at 2θ values of 30.55, 35.9, 43.6, 53.9, 57.5, and 62.4 can be attributed to the diffraction patterns of crystallographic planes (hkl) with Miller indices of (220), (311), (400), (422), (511), and (440), respectively. The present study examines the crystal faces inside the spinel structure of γ-Fe$_2$O$_3$.

The obtained result demonstrates a high level of agreement with the XRD patterns of maghemite nanoparticles, as previously published by Wu and Gao (45). The crystallite size of MNPs was determined using Scherer's Equation 2:

$$D = \frac{K*\lambda}{\beta*\cos\theta} \tag{2}$$

where D is the crystallite's mean size (nm), K is the crystallite's form factor (around 0.9 for magnetite and maghemite (dimensionless) (49), λ is the X-ray wavelength (nm), β is the FWHM (radians), and θ is the XRD angle (degrees). The crystallite size of MNPs is (11.1 nm) using Scherer's equation and the FWHM values of the most strong peaks obtained from XRD.

The SEM and TEM images of the γ-Fe$_2$O$_3$ nanoparticles were presented in Figures 4 and 5 to

Figure 2. Schematic representation of gravimetric oil spill removal
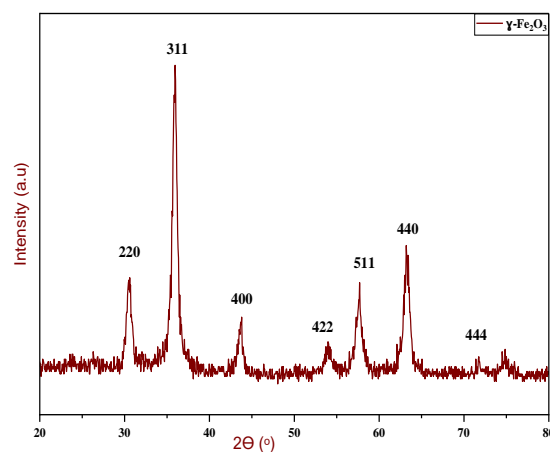

Figure 3. XRD pattern of maghemite nanoparticles

visually depict the shape of the nanoparticles and provide information on their particle size distribution. Based on the (SEM) pictures, it can be shown that the nanoparticles tended to adhere to one another, resulting in the formation of agglomerates, ultimately assuming a spherical morphology (refer to Figure 4).

The TEM picture demonstrates the presence of ultrafine particles with irregular forms (Figure 5). Based on the diminutive dimensions of particles, it can be posited that their morphology exhibits a dot-encircled, nearly spherical configuration. The particle size distribution analysis indicates that the particles are dispersed throughout a range of approximately 5-17 nm, with an average size of around 11.1 nm. The particle sizes detected in the (TEM) micrograph were consistent with the (XRD) analysis results. The particles exhibit a mostly spherical morphology and tend to overlap, forming an aggregated structure.

The presence of peaks corresponding to iron (Fe) and oxygen (O) in the EDX spectra provides evidence supporting the development of maghemite nanoparticles. As shown in Table 2 and Figure 6, the observed peaks for Na and C can be attributed to distinct causes. Na peak can be attributed to inadequate washing procedures and the subsequent deposition of salt. On the other hand, the appearance of a C peak can be attributed to the existence of organic connections of urea (50).
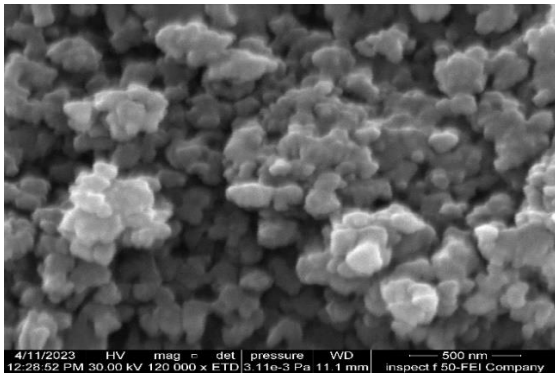
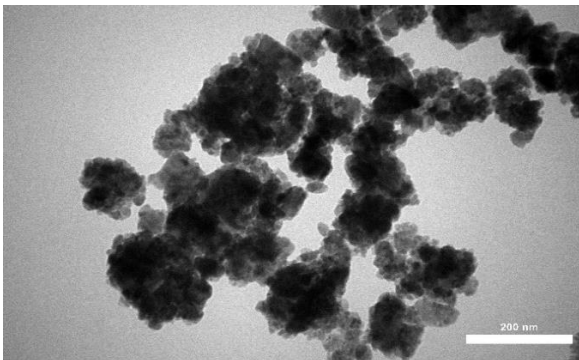**TABLE 2.** EDX pattern of maghemite nanoparticles

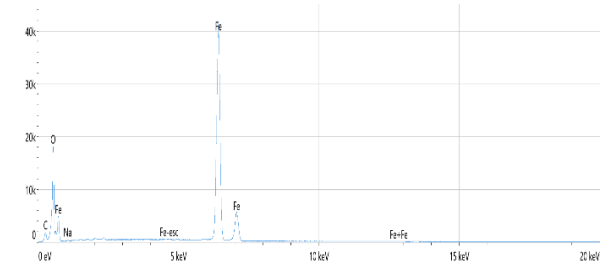| Element	Atomic %	Atomic % Error	Weight %	Weight % Error
C	13.4	0.2	5.4	0.1
O	50.6	0.3	27.3	0.2
Na	0.6	0.1	0.4	0.1
Fe	35.5	0.1	66.8	0.2

Figure 6. EDX pattern of maghemite nanoparticles

The findings obtained from the BET approach indicate that the specific surface area of MNPs was determined to be 87.01 m^2 g^{-1}. Based on the provided data, it can be inferred that the synthesized maghemite exhibits nanoparticle characteristics characterized by a very substantial specific surface area.

The magnetic properties of the synthesized maghemite magnetic nanoparticle powder were investigated using a VSM at ambient temperature. As shown in the magnetization curve of γ-Fe_2O_3 MNPs in Figure 7, which go through the zero point, and the hysteresis disappears, the remanent magnetization (Mr) and coercivity (Hc) values are very small. (Ms) are measured to be 40 emu.g^{-1}. These data mean that γ-Fe_2O_3 MNPs are super-paramagnetic (51). Super-paramagnetic nanoparticles exhibit magnetic attraction in the presence of a magnetic field but do not retain any residual magnetism once the field is removed (52).
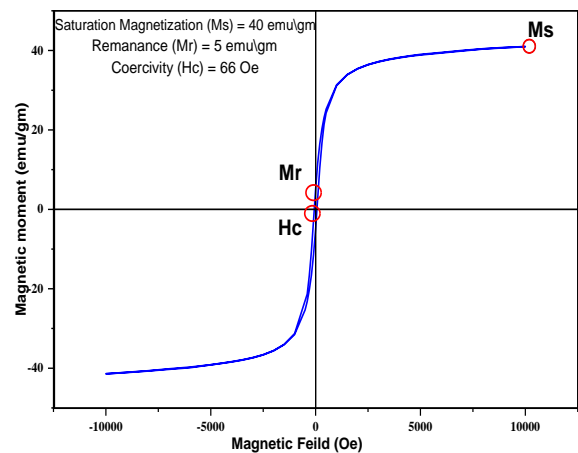

Figure 4. SEM image for maghemite nanoparticles

Figure 5. TEM image of maghemite nanoparticles

Figure 7. Magnetization curve of maghemite

Fourier transform infrared (FTIR) spectroscopy was utilized to validate the occurrence of the maghemite phase and verify the attachment of functional groups from EDTA to the surface of the iron oxide. Figure 8 displays the (FTIR) spectra of (a) pure MNPs (b) (EDTA), and (c) EDTA-coated MNPs.

The researchers suggest that the absorption band in the high wavenumber region (3600-3400) is attributed to OH stretching, while in the lower wavenumber range (700-400), it is associated with Fe-O lattice vibration (55). The curves denoted as a, b, and c exhibited maxima at wavenumbers 3427 cm^{-1}, 3417 cm^{-1}, and 3438 cm^{-1}, respectively, which can be attributed to the presence of -OH functional group. In Figure 8(a), the observed absorption peaks at 692 and 634 cm^{-1} are indicative of the presence of a Fe-O bond, which suggests the presence of γ-Fe$_2$O$_3$, as reported in the study by Bali et al. (50).

The deprotonation of the carboxyl groups of EDTA occurs during the synthesis of EDTA-MNP, where NH$_3$ and EDTA are simultaneously added. Moreover, the deprotonated carboxylate (COO-) exhibits significant asymmetric and symmetric stretching in the spectral range of 1640-1520 cm^{-1} and 1400-1300 cm^{-1}, respectively. The bands observed at wavenumbers 1628 cm^{-1} and 1430 cm^{-1} have been attributed to the asymmetric stretching (COO-) and symmetric stretching (COO-) vibrations, respectively, which is consistent with the findings reported by Shahrekizad et al. (46).

The presence of two distinct peaks within the spectral range of 2800 to 3000 cm^{-1} can be attributed to the direct correlation with the extended vibration of -CH$_2$ groups that are chelated to the γ-Fe$_2$O$_3$ compound in the EDTA complex. The grafting of EDTA onto the surface of γ-Fe$_2$O$_3$ nanoparticles has been confirmed using FTIR analysis.

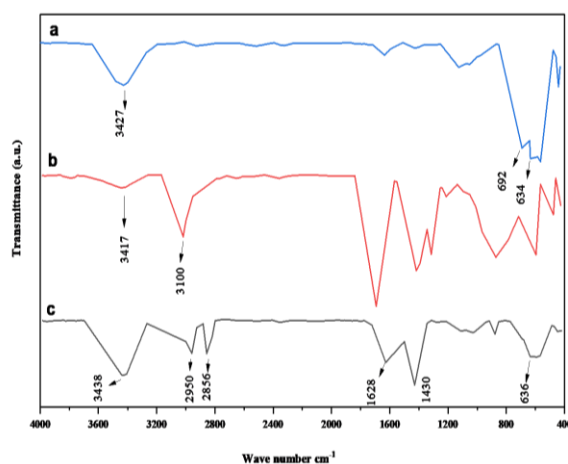**3. 2. Gravemtric Oil Removal**   This work employed three crude oil samples with varied APIs (23,28.4, and 40.3) in oil removal tests. It was noted that raising the API facilitates greater oil dispersion. The observed dispersive behavior could be attributed to the distinct chemical compositions of the oils under investigation; according to the data presented in Table 1, there is an inverse relationship between the API and the viscosity value of the oil. In other words, as the API increases, the viscosity decreases. It is plausible that oils with weaker intermolecular cohesion forces exhibit a higher degree of dispersion (53).

Oil sorption is a multifaceted phenomenon influenced by various characteristics of the oil, such as its API, density, viscosity, and adsorbent material, including its porosity and surface area (53). Figures 9 depict the impact of API on the (GOR, g/g, average values) of the oil samples under investigation, with adsorbent quantities of 0.02g and 0.06g. As evidenced, the oil with the lowest API (23) exhibited the highest (GOR) values (10.5±0.20 and 2.45±0.24 g/g), in contrast to samples with the highest APIs (28.4 and 40.3), which had a lower GOR (8.96±0.18, 1.15±0.06 and 5.11±0.15, 1.01±0.12 g/g).These results were also reported by Cardona et al. (53), their study showed a decrease in the GOR value from 11.57 ± 1.09g\g at API = 20 to 4.71 ± 0.16g\g at API = 45. These results can be attributed to the inverse relationship between API and viscosity. Lower viscosity decreases oil adherence to the adsorbent surface, resulting in reduced oil adsorption capacity (54).

Figure 10 illustrates the relationship between (GORg|g) and the quantity of adsorbent materials ranging from 0.02 g to 0.06 g. The results demonstrate a clear trend of decreasing (GOR) when the adsorbent amount increases from 0.02 to 0.06 g. Specifically, the GOR values fell from 10.5 to 2.45 g/g, 8.96 to 1.14 g/g, and 5.11 to 1.01 g/g for crude oil samples with (APIs) 23, 28.4, and 40.3, respectively.

This decrease in the oil adsorption capacity (g/g) with the increase in the adsorbent amount was also reported
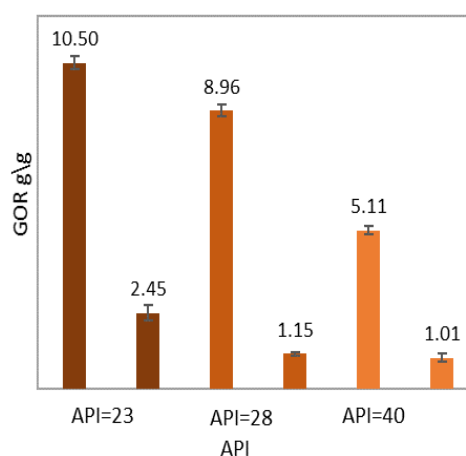
Figure 8. FTIR spectra of (a)Maghemite (b) EDTA (c) EDTA-maghemite

Figure 9. Dependence of GOR on the tested oil (at m$_1$=0.02and 0.06)

By (47, 54-56) for the oil removal employing composite based on magnetic nanoparticles. For instance, Amar et al. (47) reported a decrease in diesel engine sorption capacity from 27.65 to 7.42 g/g by increasing the mass of $ZnFe_2O_4$ MNPs from 0.01 to 0.05g. The observed decline in adsorption capacity may be due to the aggregation of the adsorbent. Consequently, the sorbent's surface area experienced a reduction, thereby impeding the infiltration of oil spills into the interior pores that are accessible for oil sorption (57).

The high GOR of EDTA-maghemite nanoparticles can be attributed to their nanosize and low density, which allow them to float with the oil on the water surface. Additionally, organic species (EDTA) enhanced the dispersion of iron oxide particles and facilitated penetration into the oil. The high surface area of maghemite nanoparticles led to high adsorption, and the super-paramagnetic properties of maghemite nanoparticles allowed for easy removal using an external
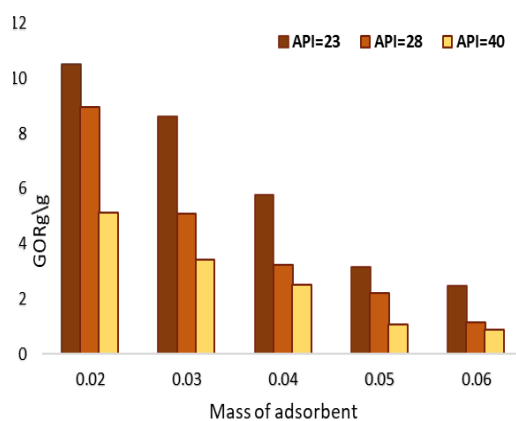

Figure 10. Relationship between the mass of EDTA-maghemite and the GOR

TABLE 3. Comparison of the gravimetric oil removal for various magnetic sorbents, based on published literature

Material	Type of oil	Gravimetric oil removal (g/g)	Reference
Fe_3O_4	Crude oil	2.16	(58)
Fe_3O_4/PS	Diesel	2.495	(59)
$PS-SIO_2$	Diesel	3	(54)
$Fe_3O_4/Silica$	Diesel	3.78	(60)
$PVDF/ CoFe_2O_4$	Decane	9.7	(61)
EDTA-γ-Fe_2O_3	Crude oil API=23	10.5±0.2-2.45±0.24	This study
EDTA-γ-Fe_2O_3	Crude oil API=28	8.96±0.18-1.15±0.06	This study
EDTA-γ-Fe_2O_3	Crude oil API=40	5.11±015- 1.01±0.12	This study

magnetic field (13). Based on published research, Table 3 a comparison of how well different magnetic sorbents remove oil using gravimetric methods.

4. CONCLUSIONS

γ-Fe_2O_3 MNPs were successfully synthesized using a homogeneous co-precipitation process at a temperature of 80°C. The XRD and FTIR analyses conducted on the magnetic nanoparticles (MNPs) provided evidence of the presence of the maghemite phase.

The determined crystallite size was approximately 11.1 nm. The particle sizes observed in the micrographs acquired from the TEM and SEM tests were consistent with the results obtained from XRD analysis. According to the SEM image, the particles exhibit a mostly spherical morphology.

The super-paramagnetic character of the synthesized maghemite was confirmed using the VSM test, resulting in improved oil separation efficiency using the magnetic separation technique. The BET analysis revealed that the synthesized maghemite exhibited a comparatively high specific surface area of 87.01 $m^2\ g^{-1}$.

The resulting MNPs were then coated with EDTA. FTIR was employed to confirm the presence of functional groups of EDTA on the iron oxide surface. The analysis revealed that the crystal structure of maghemite remained unaltered.

The coated MNPs exhibited a high adsorption capacity (GORg|g) and effectively removed oil spills from water surfaces. GOR experiments were conducted at room temperature using three crude oil samples with different (APIs) (23, 28.4, and 40.3). The results indicated that the crude oil sample with the lowest API gravity (23) exhibited the highest values of oil removal efficiency (10.5 and 2.45 g/g) when treated with adsorbents weighing 0.02 and 0.06 g, respectively; in contrast, the samples with higher APIs displayed lower oil removal efficiencies. The research findings also indicate that the quantity of adsorbent significantly impacts the (GOR), which decreased across all samples as the quantity of adsorbent increased from 0.02 to 0.06 g.

EDTA-Maghemite's small nanosize, high surface area, paramagnetic properties, low toxicity, biocompatibility, and low cost, as well as its ease of preparation, application, and separation, make it a promising adsorbent for future research to remove other petroleum derivatives and investigate the feasibility of practical use.

4. REFERENCES:

1.   Ibrahim HM. Study the optimization of petroleum refinery wastewater treatment by successive electrocoagulation and electro-oxidation systems. Iraqi Journal of Chemical and

Petroleum Engineering. 2022;23(1):31-41. https://doi.org/10.31699/IJCPE.2022.1.5

2. Makki HF, Al-Alawy AF, Al-Hassani MH, Rashad ZW. Membranes separation process for oily wastewater treatment. Journal of Engineering. 2011;17(02):235-52. 10.31699/IJCPE

3. Nguyen TG, Huynh NTH. Characterization of groundwater quality and human health risk assessment. Civil Engineering Journal. 2023;9(3):618-28. 10.28991/CEJ-2023-09-03-09

4. Aneke F, Adu J. Adsorption of heavy metals from contaminated water using leachate modular tower. Civil Engineering Journal. 2023;9(6):1522-41. 10.28991/CEJ-2023-09-06-017

5. Munasir N, Lutfiana S, Nuhaa F, Evi S, Lydia R, Ezaa S, et al. Graphene Based Membrane Modified Silica Nanoparticles for Seawater Desalination and Wastewater Treatment: Salt Rejection and Dyes. International Journal of Engineering. 2023;36(4):698-708. 10.5829/IJE.2023.36.04A.09

6. Salman RH, Abbar AH. Optimization of a combined electrocoagulation-electro-oxidation process for the treatment of Al-Basra Majnoon Oil field wastewater: Adopting a new strategy. Chemical Engineering and Processing-Process Intensification. 2023;183:109227. https://doi.org/10.1016/j.cep.2022.109227

7. Samba MA, Amar IA, Abuadabba M, ALfroji MA, Salih ZM, Erfando T, editors. Separation of crude oil and its derivatives spilled in seawater by using cobalt ferrite oxide. Second International Conference on Science, Engineering and Technology (ICoSET 2019), Universitas Islam Riau, Pekanbaru, Indonesia; 2020.

8. Rashdan SA, Hazeem LJ. Synthesis of spinel ferrites nanoparticles and investigating their effect on the growth of microalgae Picochlorum sp. Arab Journal of Basic and Applied Sciences. 2020;27(1):134-41. https://doi.org/10.1080/25765299.2020.1733174

9. Elias E, Costa R, Marques F, Oliveira G, Guo Q, Thomas S, et al. Oil-spill cleanup: The influence of acetylated curaua fibers on the oil-removal capability of magnetic composites. Journal of Applied Polymer Science. 2015;132(13). https://doi.org/10.1002/app.41732

10. Mendes MDSL, Coutinho LCDS, Araujo AB, Neves MAFES, Pedrosa MS. Comprehensive review of magnetic polymeric nanocomposites with superparamagnetic iron oxide nanoparticles for oil remov-al from water. https://doi.org/10.37358/RC.23.1.8562

11. Guerra FD, Attia MF, Whitehead DC, Alexis F. Nanotechnology for environmental remediation: materials and applications. Molecules. 2018;23(7):1760. https://doi.org/10.3390/molecules23071760

12. Kharisov BI, Dias HR, Kharissova OV. Nanotechnology-based remediation of petroleum impurities from water. Journal of Petroleum Science and Engineering. 2014;122:705-18. https://doi.org/10.1016/j.petrol.2014.09.013

13. Mohamed NH, Aljaafari A. Synthesis of magnetic nanoparticles and nanosheets for oil spill. Nanoscience and Nanotechnology-Asia. 2015;5(1):32-43. 10.2174/2210681205666150601215445

14. de Andrade JR, Oliveira MF, da Silva MG, Vieira MG. Adsorption of pharmaceuticals from water and wastewater using nonconventional low-cost materials: a review. Industrial & Engineering Chemistry Research. 2018;57(9):3103-27. https://doi.org/10.1021/acs.iecr.7b05137

15. Yandri Y, Ropingi H, Suhartati T, Irawan B, Hadi S. Immobilization of Aspergillus fumigatus α-Amylase via Adsorption onto Bentonite/Chitosan for Stability Enhancement. Emerging Science Journal. 2023;7(5):1811-26. https://doi.org/10.31699/IJCPE.2017.1.6

16. Al-Alawy AF, Al-Ameri MK. Treatment of simulated oily wastewater by ultrafiltration and nanofiltration processes. Iraqi Journal of Chemical and Petroleum Engineering. 2017;18(1):71-85. https://doi.org/10.1063/5.0151527

17. Mnaty KH, Saleem AM, editors. Using the nanotechnology method to remove oil spill pollution of water. AIP Conference Proceedings; 2023: AIP Publishing.

18. Akrami A, Niazi A. Synthesis of maghemite nanoparticles and its application for removal of Titan yellow from aqueous solutions using full factorial design. Desalination and Water Treatment. 2016;57(47):22618-31. https://doi.org/10.5004/dwt.2018.22456

19. Kadhim RM, Al-Abodi EE, Al-Alawy AF. Citrate-coated magnetite nanoparticles as osmotic agent in a forward osmosis process. Desalination and Water Treatment. 2018;115:45-52. 10.30638/eemj.2015.135

20. Stoia M, Muntean C. Preparation, characterization and adsorption properties of MFE 2 o 4 (m= Ni, Co, Cu) nanopowders. Environmental Engineering & Management Journal (EEMJ). 2015;14(6). 10.30638/eemj.2015.135

21. Tronc E, Ezzir A, Cherkaoui R, Chanéac C, Noguès M, Kachkachi H, et al. Surface-related properties of γ-Fe2O3 nanoparticles. Journal of Magnetism and Magnetic Materials. 2000;221(1-2):63-79. https://doi.org/10.1016/S0304-8853(00)00369-3

22. Li P, Yu B, Wei X. Synthesis and characterization of a high oil-absorbing magnetic composite material. Journal of applied polymer science. 2004;93(2):894-900. https://doi.org/10.1002/app.20522

23. Majeed NS, Naji DM. Synthesis and characterization of iron oxide nanoparticles by open vessel ageing process. Iraqi Journal of Chemical and Petroleum Engineering. 2018;19(2):27-31. https://doi.org/10.31699/IJCPE.2018.2.5

24. Shariatzadeh S, Salimi M, Fathinejad H, Hassani Joshaghani A. Nanostructured α-Fe2O3: Solvothermal synthesis, characterization, and effect of synthesis parameters on structural properties. International Journal of Engineering, Transactions B: Applications. 2022;35(6):1186-92. 10.5829/IJE.2022.35.06C.10

25. Ko S, Kim ES, Park S, Daigle H, Milner TE, Huh C, et al. Amine functionalized magnetic nanoparticles for removal of oil droplets from produced water and accelerated magnetic separation (Retraction of Vol 19, art no 132, 2017). SPRINGER VAN GODEWIJCKSTRAAT 30, 3311 GZ DORDRECHT, NETHERLANDS; 2021.

26. Cornell RM, Schwertmann U. The iron oxides: structure, properties, reactions, occurrences, and uses: Wiley-vch Weinheim; 2003.

27. Muldarisnur M, Perdana I, Elvaswer E, Puryanti D. Mapping of sensing performance of concentric and non-concentric silver nanoring. Emerging Science Journal. 2023;7(4):1083-99. 10.28991/ESJ-2023-07-04-04

28. Adewunmi AA, Kamal MS, Solling TI. Application of magnetic nanoparticles in demulsification: A review on synthesis, performance, recyclability, and challenges. Journal of Petroleum Science and Engineering. 2021;196:107680. https://doi.org/10.1016/j.petrol.2020.107680

29. Ali AF, Atwa SM, El-Giar EM. Development of magnetic nanoparticles for fluoride and organic matter removal from drinking water. Water Purification: Elsevier; 2017. p. 209-62.

30. Thakor AS, Jokerst JV, Ghanouni P, Campbell JL, Mittra E, Gambhir SS. Clinically approved nanoparticle imaging agents. Journal of Nuclear Medicine. 2016;57(12):1833-7. 10.2967/jnumed.116.181362

31. Shokrollahi H. Structure, synthetic methods, magnetic properties and biomedical applications of ferrofluids. Materials Science and Engineering: C. 2013;33(5):2476-87. https://doi.org/10.1016/j.msec.2013.03.028

32. Sun X, Zhang Y, Chen G, Gai Z. Application of nanoparticles in enhanced oil recovery: a critical review of recent progress. Energies. 2017;10(3):345. https://doi.org/10.3390/en10030345

33. Natarajan S, Harini K, Gajula GP, Sarmento B, Neves-Petersen MT, Thiagarajan V. Multifunctional magnetic iron oxide nanoparticles: Diverse synthetic approaches, surface modifications, cytotoxicity towards biomedical and industrial applications. BMC Materials. 2019;1(1):1-22. 10.1186/s42833-019-0002-6

34. Salman K. synthesis and characterization unsaturated polyester resin nanocomposites reinforced by Fe2O3+ Ni nanoparticles: Influence on mechanical and magnetic properties. International Journal of Engineering, Transactions A: Basics. 2022;35(1):21-8. 10.5829/IJE.2022.35.01A.03

35. Serrano-Ruiz D, Laurenti M, Ruiz-Cabello J, López-Cabarcos E, Rubio-Retama J. Hybrid microparticles for drug delivery and magnetic resonance imaging. Journal of Biomedical Materials Research Part B: Applied Biomaterials. 2013;101(4):498-505. https://doi.org/10.1002/jbm.b.32792

36. Stamatis H, Taha AA, Al-Jawad SM, Yousif NA. A review of structure, properties, and chemical synthesis of magnetite nanoparticles. Journal of Applied Sciences and Nanotechnology. 2023;3(2). https://doi.org/10.53293/jasn.2022.5179.1178

37. Cheng Z, Tan ALK, Tao Y, Shan D, Ting KE, Yin XJ. Synthesis and characterization of iron oxide nanoparticles and applications in the removal of heavy metals from industrial wastewater. International Journal of Photoenergy. 2012;2012. https://doi.org/10.1155/2012/608298

38. Passow U, Lee K. Future oil spill response plans require integrated analysis of factors that influence the fate of oil in the ocean. Current Opinion in Chemical Engineering. 2022;36:100769. https://doi.org/10.1016/j.coche.2021.100769

39. Loyeh EN, Mohsenpour R. Investigation of oil pollution on aquatic animals and methods of its prevention. J Aquac Mar Biol. 2020;9(5):160-5. 10.15406/jamb.2020.09.00291

40. Jawad AS, Al-Alawy AF, editors. Synthesis and characterization of coated magnetic nanoparticles and its application as coagulant for removal of oil droplets from oilfield produced water. AIP Conference Proceedings; 2020: AIP Publishing.

41. Ramos-Guivar JA, Lopez EO, Greneche J-M, Litterst FJ, Passamani EC. Effect of EDTA organic coating on the spin canting behavior of maghemite nanoparticles for lead (II) adsorption. Applied Surface Science. 2021;538:148021. https://doi.org/10.1016/j.apsusc.2020.148021

42. Liu Y, Chen M, Yongmei H. Study on the adsorption of Cu (II) by EDTA functionalized Fe3O4 magnetic nano-particles. Chemical Engineering Journal. 2013;218:46-54. https://doi.org/10.1016/j.cej.2012.12.027

43. Sandoval-Cárdenas DI, Pool H, Favela-Camacho SE, Santos-Cruz J, Campos-Guillén J, Ramos-López MA, et al. Sargassum@ magnetite composite EDTA-functionalized for the potential removal of mercury. Polymers. 2023;15(6):1405. https://doi.org/10.3390/polym15061405

44. Khelifa A, Aoudj S, Moulay S, De Petris-Wery M. A one-step electrochlorination/electroflotation process for the treatment of heavy metals wastewater in presence of EDTA. Chemical Engineering and Processing: Process Intensification. 2013;70:110-6. https://doi.org/10.1016/j.cep.2013.04.013

45. Wu Z-G, Gao J-F. Synthesis of γ-Fe2O3 nanoparticles by homogeneous co-precipitation method. Micro & Nano Letters. 2012;7(6):533-5. 10.1049/mnl.2012.0310

46. Shahrekizad M, GHOLAMALIZADEH AA, Mir N. EDTA-coated Fe3O4 nanoparticles: a novel biocompatible fertilizer for improving agronomic traits of sunflower (Helianthus annuus). 2015. 10.7508/JNS.2015.02.006

47. Amar IA, Alzarouq A, Mohammed W, Zhang M, Matroed N. Oil spills removal from seawater surface by magnetic biochar composite derived from Heglig tree bark and cobalt ferrite. World Journal of Engineering. 2023(ahead-of-print). http://doi.org/10.1108/WJE-11-2022-0459

48. Sreeja V, Joy P. Microwave–hydrothermal synthesis of γ-Fe2O3 nanoparticles and their magnetic properties. Materials Research Bulletin. 2007;42(8):1570-6. https://doi.org/10.1016/j.materresbull.2006.11.014

49. Afkhami A, Moosavi R. Adsorptive removal of Congo red, a carcinogenic textile dye, from aqueous solutions by maghemite nanoparticles. Journal of hazardous materials. 2010;174(1-3):398-403. https://doi.org/10.1016/j.jhazmat.2009.09.066

50. Bali Ogholbeyg A, Kianvash A, Hajalilou A, Abouzari-Lotf E, Zarebkohan A. Cytotoxicity characteristics of green assisted-synthesized superparamagnetic maghemite (γ-Fe 2 O 3) nanoparticles. Journal of Materials Science: Materials in Electronics. 2018;29:12135-43. 10.1007/s10854-018-9321-8

51. Aliahmad M, Nasiri Moghaddam N. Synthesis of maghemite (γ-Fe 2 O 3) nanoparticles by thermal-decomposition of magnetite (Fe 3 O 4) nanoparticles. Materials Science-Poland. 2013;31:264-8.

52. Alibeigi S, Vaezi MR. Phase transformation of iron oxide nanoparticles by varying the molar ratio of Fe2+: Fe3+. Chemical Engineering & Technology: Industrial Chemistry-Plant Equipment-Process Engineering-Biotechnology. 2008;31(11):1591-6. https://doi.org/10.1002/ceat.200800093

53. Cardona D, Debs K, Lemos S, Vitale G, Nassar N, Carrilho E, et al. A comparison study of cleanup techniques for oil spill treatment using magnetic nanomaterials. Journal of environmental management. 2019;242:362-71. https://doi.org/10.1016/j.jenvman.2019.04.106

54. Damavandi F, Soares JB. Polystyrene magnetic nanocomposite blend: an effective, facile, and economical alternative in oil spill removal applications. Chemosphere. 2022;286:131611. https://doi.org/10.1016/j.chemosphere.2021.131611

55. Silveira Maranhão Fd, Gomes F, Thode S, Das DB, Pereira E, Lima N, et al. Oil spill sorber based on extrinsically magnetizable porous geopolymer. Materials. 2021;14(19):5641. 10.3390/ma14195641

56. Gomes de Souza Jr F, Marins JA, Rodrigues CH, Pinto JC. A magnetic composite for cleaning of oil spills on water. Macromolecular Materials and Engineering. 2010;295(10):942-8. https://doi.org/10.1002/mame.201000090

57. Amar I, Alshibani Z, AbdulQadir M, Abdalsamed I, Altohami F. Oil spill removal from water by absorption on zinc-doped cobalt ferrite magnetic nanoparticles. Advanced Journal of Chemistry-Section A. 2019;2(4):365-76. 10.2174/2210681205666150601215445

58. Debs KB, Cardona DS, da Silva HD, Nassar NN, Carrilho EN, Haddad PS, et al. Oil spill cleanup employing magnetite nanoparticles and yeast-based magnetic bionanocomposite. Journal of environmental management. 2019;230:405-12. https://doi.org/10.1016/j.jenvman.2018.09.094

59. Yu L, Hao G, Gu J, Zhou S, Zhang N, Jiang W. Fe3O4/PS magnetic nanoparticles: Synthesis, characterization and their application as sorbents of oil from waste water. Journal of Magnetism and Magnetic Materials. 2015;394:14-21. https://doi.org/10.1016/j.jmmm.2015.06.045

60. Yu L, Hao G, Liang Q, Zhou S, Zhang N, Jiang W. Facile preparation and characterization of modified magnetic silica nanocomposite particles for oil absorption. Applied Surface Science. 2015;357:2297-305. https://doi.org/10.1016/j.apsusc.2015.09.231

61. Dorneanu PP, Cojocaru C, Olaru N, Samoila P, Airinei A, Sacarescu L. Electrospun PVDF fibers and a novel PVDF/CoFe2O4 fibrous composite as nanostructured sorbent materials for oil spill cleanup. Applied Surface Science. 2017;424:389-96. https://doi.org/10.1016/j.apsusc.2017.01.177

Persian Abstract

چکیده

نشت نفت چالش های زیست محیطی، اکولوژیکی و اقتصادی قابل توجهی در سراسر جهان ایجاد می کند. از آنجایی که فناوری‌های اصلاحی فعلی در احیای اکوسیستم‌های دریایی ناکارآمد هستند، این مطالعه یک روش ساده و مقرون به صرفه برای استفاده از نانوذرات مغناطیسی اکسید آهن را اتخاذ کرد. نانوذرات مغناطیسی ماگمیت (γ-Fe2O3) (MNPs) با استفاده از روش همگن رسوب دهی سنتز شدند. پراکندگی کلوئیدی MNP ها با اعمال یک پوشش اتیلن دی آمین ترا استیک اسید (EDTA)افزایش یافت که منجر به کاهش انرژی سطحی بالا و کاهش متعاقب آن در تجمع نانوذرات شد. MNPها با استفاده از پراش پرتو ایکس (XRD)، طیف‌سنجی فروسرخ تبدیل فوریه (FTIR)، میکروسکوپ الکترونی عبوری (TEM)، میکروسکوپ الکترونی روبشی (SEM)، طیف‌سنجی پرتو ایکس پراکنده انرژی (EDX)و مغناطیس‌سنج نمونه ارتعاشی (EDX) مشخص شدند. (VSM).آزمایش های حذف در دمای ۲۵ درجه سانتی گراد با محدوده جرمی جاذب (۰.۰۶-۰.۰۲ گرم) انجام شد. نانوذرات مغناطیسی آلوده به نفت توسط یک میدان مغناطیسی خارجی با استفاده از آهنربای نئودیمیم از سطح آب استخراج شدند. اثرات API روغن و جرم جاذب بر حذف روغن گرانشی (GOR)مورد بررسی قرار گرفت. GOR برای API های ۲۳، ۲۸.۴ و ۴۰.۳ به ترتیب ۰.۲۴±۲.۴۵-۰.۲.۲±۱۰.۵، ۱.۱۵±۰.۰۶، ۸.۹۶±۰.۱۸±۱.۱۵±۰.۰۶ و ۵.۱۱±۱.۱۵±۰.۰۶ تا ۱.۰۱±۰.۱۲ گرم بر گرم بود. نتایج تجربی یک رابطه معکوس بین GOR و مقدار API را نشان داد، که نشان می‌دهد با کاهش مقدار API، GOR افزایش می‌یابد و بالعکس. علاوه بر این، با افزایش جرم ماده جاذب (۰.۰۶-۰.۰۲ گرم)، مقدار GOR کاهش یافت. نتایج این مطالعه نشان می‌دهد که MNPهای EDTA-maghemite دارای ویژگی‌های سودمندی از جمله اندازه نانو کوچک، رفتار فوق‌پارامغناطیس و سطح بزرگ هستند. این ویژگی ها EDTA-maghemite را به یک جاذب مناسب برای از بین بردن نشت نفت از سطوح آب تبدیل می کند.